Astronomy
&
Astrophysics

The HARPS search for southern extra-solar planets

X. A *m* sin *i* = 11 *M*$_\oplus$ planet around the nearby spotted M dwarf GJ 674[*],[**]

X. Bonfils[1], M. Mayor[2], X. Delfosse[3], T. Forveille[3], M. Gillon[2], C. Perrier[3], S. Udry[2], F. Bouchy[4], C. Lovis[2], F. Pepe[2], D. Queloz[2], N. C. Santos[1,2,5], and J.-L. Bertaux[6]

[1] Centro de Astronomia e Astrofísica da Universidade de Lisboa, Observatório Astronómico de Lisboa, Tapada da Ajuda, 1349-018 Lisboa, Portugal
e-mail: xavier.bonfils@oal.ul.pt
[2] Observatoire de Genève, 51 ch. des Maillettes, 1290 Sauverny, Switzerland
[3] Laboratoire d'Astrophysique, Observatoire de Grenoble, Université J. Fourier, BP 53, 38041 Grenoble, Cedex 9, France
[4] Institut d'Astrophysique de Paris, CNRS, Université Pierre et Marie Curie, 98bis Bd Arago, 75014 Paris, France
[5] Centro de Astrofísica, Universidade do Porto, Rua das Estrelas, 4150-762 Porto, Portugal
[6] Service d'Aéronomie du CNRS, BP 3, 91371 Verrières-le-Buisson, France

ABSTRACT

Context. How planet properties depend on stellar mass is a key diagnostic of planetary formation mechanisms.
Aims. This motivates planet searches around stars that are significantly more massive or less massive than the Sun, and in particular our radial velocity search for planets around very low-mass stars.
Methods. As part of that program, we obtained measurements of GJ 674, an M 2.5 dwarf at $d = 4.5$ pc. These measurements have dispersion much in excess of their internal errors. An intensive observing campaign demonstrates that the excess dispersion is due to two superimposed coherent signals, with periods of 4.69 and 35 days.
Results. These data are described well by a 2-planet Keplerian model where each planet has a ∼11 $M_\oplus$ minimum mass. A careful analysis of the (low-level) magnetic activity of GJ 674, however, demonstrates that the 35-day period coincides with the stellar rotation period. This signal therefore originates in a spot inhomogeneity modulated by stellar rotation. The 4.69-day signal, on the other hand, is caused by a bona-fide planet, GJ 674b.
Conclusions. Its detection adds to the growing number of Neptune-mass planets around M-dwarfs and reinforces the emerging conclusion that this mass domain is much more populated than the Jovian mass range. We discuss the metallicity distributions of M dwarf *with* and *without* planets and find a low 11% probability that they are drawn from the same parent distribution. Moreover, we find tentative evidence that the host star metallicity correlates with the total mass of their planetary system.

Key words. stars: individual: GJ 674 – stars: planetary systems – stars: late-type – techniques: radial velocities

1. Introduction

The M dwarfs, the most common stars in our Galaxy, were added to the target lists of planet-search programs soon after the first exoplanet discoveries. Compared to Sun-like stars, they suffer from some drawbacks: they are faint so photon noise often limits measurements of their radial velocity, and many are at least moderately active and thus prone to so-called "radial-velocity jitter" (Saar & Donahue 1997). On the other hand, the lower masses of M dwarfs result in a higher wobble amplitude for a given planetary mass, and their p-mode oscillations have both smaller amplitudes and shorter periods than those of solar type stars. These oscillations therefore average out much faster. As a result, the detection of an Earth-like planet in the – closer – habitable zone of an M dwarf is actually within reach of today's

best spectrographs. Perhaps most important, however, M dwarfs represent unique targets for probing the dependence on the stellar mass of planetary formation, thanks to the wide mass range (0.1 to 0.6 $M_\odot$) spanned by that spectral class alone.

The first planet found to orbit an M dwarf, GJ 876b (Delfosse et al. 1998; Marcy et al. 1998), was only the 9th exoplanet discovered around a main sequence star. Besides showing that Jupiter-mass planets can form at all around very low-mass stars, its discovery suggested that they might be common, since it was found amongst the few dozen M dwarfs that were observed at that time. Despite these early expectations, no other M dwarf was reported hosting a planet until 2004, though a second planet (GJ 876c, $m_p \sin i = 0.56$ M_{Jup} – Marcy et al. 2001) was soon found around GJ 876 itself.

In 2004, the continuous improvement of the radial-velocity techniques resulted in the quasi-simultaneous discovery of three Neptune-mass planets around μ Ara ($m_p \sin i = 14$ $M_\oplus$ – Santos et al. 2004), ρ Cnc ($m_p \sin i = 14$ $M_\oplus$ – McArthur et al. 2004), and GJ 436 ($m_p \sin i = 23$ $M_\oplus$ – Butler et al. 2004; Maness et al. 2006). Of those three, GJ 436b orbits an M dwarf, which put that spectral class back on the discovery forefront. It was soon followed by another two: a single planet around GJ 581

($m_p \sin i = 17\ M_\oplus$ – Bonfils et al. 2005b) and a very light ($m_p = 7.5\ M_\oplus$) third planet in the GJ 876 system (Rivera et al. 2005). As a result, planets around M dwarfs today represent a substantial fraction (30%) of all known planets with $m \sin i \lesssim 30\ M_\oplus$.

Even with GJ 849b ($m_p \sin i = 0.82\ M_{\rm Jup}$ – Butler et al. 2006) now completing the inventory of M-dwarf planets found with radial-velocity techniques, the upper range of planet masses remains scarcely populated. This contrasts both with the (still very incompletely known) Neptune-mass planets orbiting M dwarfs and with the Jovian planets around Sun-like stars. At larger separations, microlensing surveys similarly probe the frequency of planets as a function of their mass. That technique has detected four putative planets that are probably orbiting M dwarfs : OGLE235-MOA53b ($m_p \sim 2.6\ M_{\rm Jup}$ – Bond et al. 2004; Bennett et al. 2006), OGLE-05-071Lb ($m_p = 0.9\ M_{\rm Jup}$ – Udalski et al. 2005), OGLE-05-390Lb ($m_p = 0.017\ M_{\rm Jup}$ – Beaulieu et al. 2006), and OGLE-05-169Lb ($m_p = 0.04\ M_{\rm Jup}$ – Gould et al. 2006). Two of these four planets very likely have masses below $0.1\ M_{\rm Jup}$. Given the detection bias of that technique towards massive companions, this again suggests that Neptune-mass planets are much more common than Jupiter-mass ones around very low-mass stars.

Here we report the discovery of a 11 $M_\oplus$ planet orbiting GJ 674 every 4.69 days. GJ 674b has the 5th lowest mass of the known planets, and coincidentally is also the 5th planetary system centered on an M dwarf. Its detection adds to the small inventory of both very low-mass planets and planets around very low-mass stars. After reviewing the properties of the GJ 674 star (Sect. 2), we briefly present our radial velocity measurements (Sect. 3) and their Keplerian analysis (Sect. 4). A careful analysis of the magnetic activity of GJ 674 (Sect. 5) assigns one of the two periodicities to rotational modulation of a stellar spot signal and the other one to a *bona fide* planet. We conclude with a brief discussion of the properties of the detected planet.

2. The properties of GJ 674

GJ 674 (HIP 85523, LHS 449) is a M 2.5 dwarf (Hawley et al. 1997) in the Altar constellation. At 4.5 pc ($\pi = 220.43 \pm 1.63$ mas – ESA 1997), it is the 37th closest stellar system, the 54th closest star (taking stellar multiplicity into account)[1] and only the 2nd closest known planetary system (after ϵ Eridani, and slightly closer than GJ 876).

Its photometry ($V = 9.382 \pm 0.012$; $K = 4.855 \pm 0.018$ – Turon et al. 1993; Cutri et al. 2003) and parallax imply absolute magnitudes of $M_V = 11.09 \pm 0.04$ and $M_K = 6.57 \pm 0.04$. GJ 674's $J - K$ color (= 0.86 – Cutri et al. 2003) and the Leggett et al. (2001) color-bolometric relation result in a K-band bolometric correction of $BC_K = 2.67$, and in a $0.016\ L_\odot$ luminosity. The K-band mass–luminosity relation of Delfosse et al. (2000) gives a $0.35\ M_\odot$ mass and the Bonfils et al. (2005a) photometric calibration of the metallicity results in [Fe/H] = -0.28 ± 0.2. The moderate X-ray luminosity ($L_x/L_{\rm bol} \simeq 5 \times 10^{-5}$ – Hünsch et al. 1999) and Ca II H & K emission depict a modestly active M dwarf (Fig. 1). Its UVW galactic velocities place GJ 674 between the young and old disk populations (Leggett 1992), suggesting an age of $\sim 10^{8-9}$ yr.

Last but not least, since we are concerned with radial velocities, the high proper motion of GJ 674 (1.05 arcsec yr^{-1} – ESA 1997) changes the orientation of its velocity vector along the line
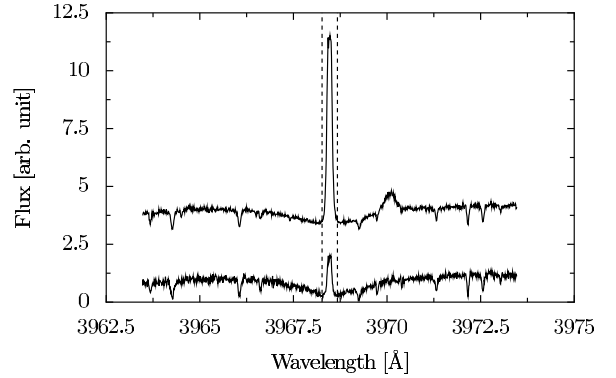
---
[1] On 2007 Mar. 1 (http://www.chara.gsu.edu/RECONS/TOP100.htm).

Fig. 1. Emission reversal in the Ca II H line of GJ 674 (*top*) and GJ 581 (*bottom*). Within our sample, GJ 581 has one of the weakest Ca II emissions and illustrates a very quiet M dwarf. GJ 674 has much stronger emission and is moderately active.

Table 1. Observed and inferred stellar parameters for GJ 674.

Parameter		GJ 674
Spectral type		M 2.5
V		9.382 ± 0.012
π	[mas]	220.43 ± 1.63
Distance	[pc]	4.54 ± 0.03
M_V		11.09 ± 0.04
K		4.855 ± 0.018
M_K		6.57 ± 0.04
$L_\star$	[$L_\odot$]	0.016
$L_x/L_{\rm bol}$		5×10^{-5}
$v \sin i$	[km s^{-1}]	$\lesssim 1$
dv_r/dt	[m s^{-1} yr^{-1}]	0.115
[Fe/H]		-0.28
$M_\star$	[$M_\odot$]	0.35
age	[Gyr]	0.1-1
$T_{\rm eff}$	[K]	3500–3700

of sight (e.g. Kürster et al. 2003) to result in an apparent secular acceleration of 0.115 m s^{-1} yr^{-1}. At our current precision, this acceleration will not be detectable before another decade.

3. Radial-velocity data

We observed GJ 674 with the HARPS echelle spectrograph (Mayor et al. 2003) mounted on the ESO 3.6-m telescope at La Silla Observatory (Chile). After demonstrating impressive planet-finding capabilities right after its commissioning (Pepe et al. 2004), this spectrograph now defines the state of the art in radial-velocity measurements, delivering a significantly better precision than its ambitious 1 m s^{-1} specification. Like one recent published example, Lovis et al. (2006) also obtained a 0.64 m s^{-1} dispersion for the residuals of their orbital solution of the 3 Neptune-mass planets of HD 69830.

We observed GJ 674 without interlaced Thorium-Argon light to obtain cleaner spectra for spectroscopic analysis, at some small cost in the ultimate Doppler precision. Since June 2004, we have gathered 32 exposures of 900 s each with a median S/N ratio of ~90. Their Doppler information content, evaluated according to the prescriptions of Bouchy et al. (2001), is mostly below 1 m s^{-1}. Our internal errors also include, in quadrature sum, an "instrumental" uncertainty of 0.5 m s^{-1} for the nightly drift of the spectrograph (since we do not use the ThAr lamp to monitor it) and the measurement uncertainty of the daily wavelength zero-point calibration. We did benefit from the recent
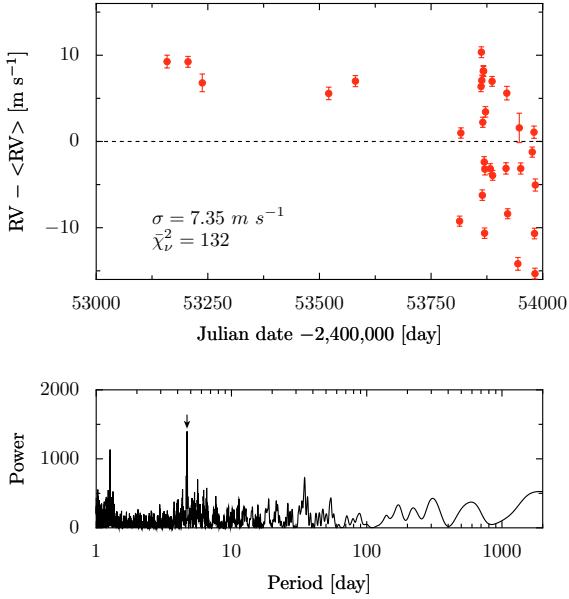
Fig. 2. *Upper panel*: radial-velocity measurements of GJ 674 as a function of time. The high dispersion ($\sigma = 7.35\,\mathrm{m\,s^{-1}}$) and chi-square value ($\bar{\chi}^2 = 132$) betray a (coherent or incoherent) signal in the data. *Bottom panel*: the Lomb-Scargle periodogram of the velocities has prominent power excess around $P = 4.69$ days (downward arrow), which indicates that much of the excess dispersion reflects a coherent signal with a period close to that value. The second-highest peak, at 1.27 day, is a one-day alias of the 4.69 day period ($1.27 \simeq 1 + 1/4.69$).

improvements in the HARPS wavelength calibration, which is now stable to $0.2\,\mathrm{m\,s^{-1}}$ (Lovis & Pepe 2007).

A constant radial velocity gives a very high reduced chi-square value ($\bar{\chi}^2 = 132$) for the time series, which reflects a dispersion ($\sim 7.4\,\mathrm{m\,s^{-1}}$) well above our internal errors (Fig. 2). This prompted a search for an orbital (Sect. 4) and/or magnetic-activity (Sect. 5) signal.

4. Orbital analysis

A Lomb-Scargle periodogram (Press et al. 1992) of the velocity measurements shows a narrow peak around 4.69-day (Fig. 2). Adjustment of a single Keplerian orbit demonstrates that it is best described by an $m_2 \sin i = 12.7\,M_\oplus$ planet ($0.040\,M_{\mathrm{Jup}}$) revolving around GJ 674 every $P_2 = 4.6940 \pm 0.0005$ days in a slightly eccentric orbit ($e_2 = 0.10 \pm 0.02$). The residuals around this low-amplitude orbit ($K_1 = 9.8 \pm 0.2\,\mathrm{m\,s^{-1}}$) have a dispersion of $3.27\,\mathrm{m\,s^{-1}}$ (Fig. 3), still well above our measurement errors, and the reduced chi-square per degree of freedom is $\bar{\chi}^2 = 30.6$. A periodogram of the residuals indicates that much of this excess dispersion stems from a broad power peak centered around 35 days, prompting us to perform a 2-planet fit.

We searched for 2-planet Keplerian solutions with *Stakanof* (Tamuz, in prep.), a program that uses genetic algorithms to efficiently explore the large parameter space of multi-planet models. *Stakanof* quickly converged to a 2-planet solution that describes our measurements much better than the single-planet fit ($\sigma = 0.82\,\mathrm{m\,s^{-1}}$, $\bar{\chi}^2 = 2.57$ per degree of freedom – Fig. 4). The orbital parameters of the 4.69-day planet change little from the 1-planet fit, except for the eccentricity, which increases to $e_2 = 0.20 \pm 0.02$. Its mass is revised down to $M_2 \sin i = 11.09\,M_\oplus$, and the period hardly changes, $P_2 = 4.6938 \pm 0.0007$ day. The second planet would have a $P_3 = 34.8467 \pm 0.0324$ day period, an $e_3 = 0.20 \pm 0.05$ eccentricity, and a minimum mass
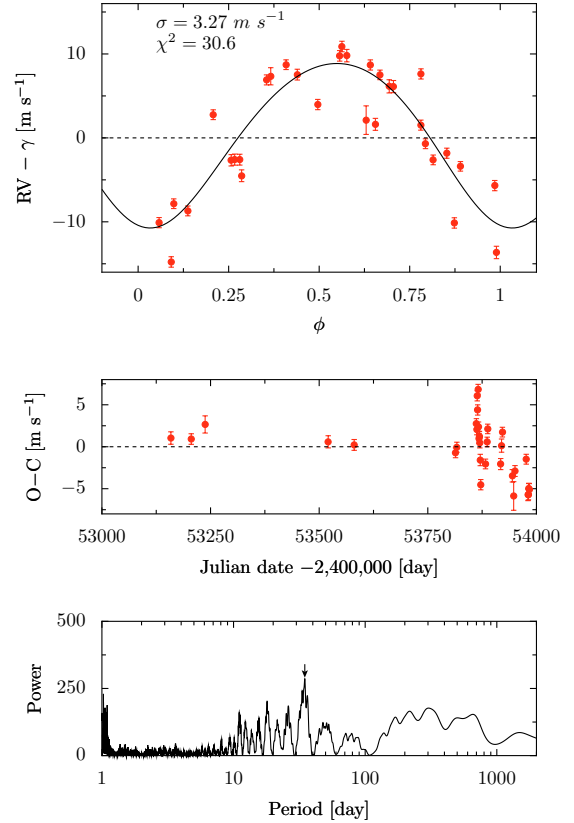

Fig. 3. *Upper panel*: radial velocities of GJ 674 (red filled circles) phase-folded to the 4.6940 days period of the best 1-planet fit (curve). The dispersion around the fit ($\sigma = 3.27\,\mathrm{m\,s^{-1}}$) and its reduced chi-square ($\bar{\chi}^2 = 30.6$ per degree of freedom) indicate that a single planet does not describe the data very well. *Middle panel*: radial-velocity residuals of the 1-planet fit *Bottom panel*: the Lomb-Scargle periodogram of the residuals shows a broad peak centered around 35 days.

of $m_3 \sin i = 12.58\,M_\oplus$. Such periods would correspond to semi-major axes of 0.04 and 0.15 AU. Those are enough disjointed that mutual interactions can be neglected over observable time scales, and that the system would be stable on longer time scales.

The low dispersion around the solution and the lack of any significant peak in the Lomb-Scargle periodogram of its residuals shows that our current radial-velocity measurements contain no evidence of an additional component.

5. Activity analysis

Apparent Doppler shifts unfortunately do not always originate in the gravitational pull of a companion: in a rotating star, stellar surface inhomogeneities such as plages and spots can break the exact balance between light emitted in the red-shifted and blue-shifted halves of the star. Observationally, these inhomogeneities translate into flux variations, as well as into changes of both the shape and the centroid of spectral lines (Saar & Donahue 1997; Queloz et al. 2001). Spots also typically impact spectral indices, whether designed to probe the chromosphere (to which photospheric spots have strong magnetic connections) or the photosphere (because spots have cooler spectra). Of the two candidate periods, the 4.69-day one is unlikely to reflect stellar rotation. From our GJ 674 spectra we measure a rotational velocity of $v \sin i \lesssim 1\,\mathrm{km\,s^{-1}}$, which would need a rather improbable stellar inclination ($i \lesssim 15°$) to match such a short period. The moderate activity level of GJ 674, on the other hand, leaves the nature
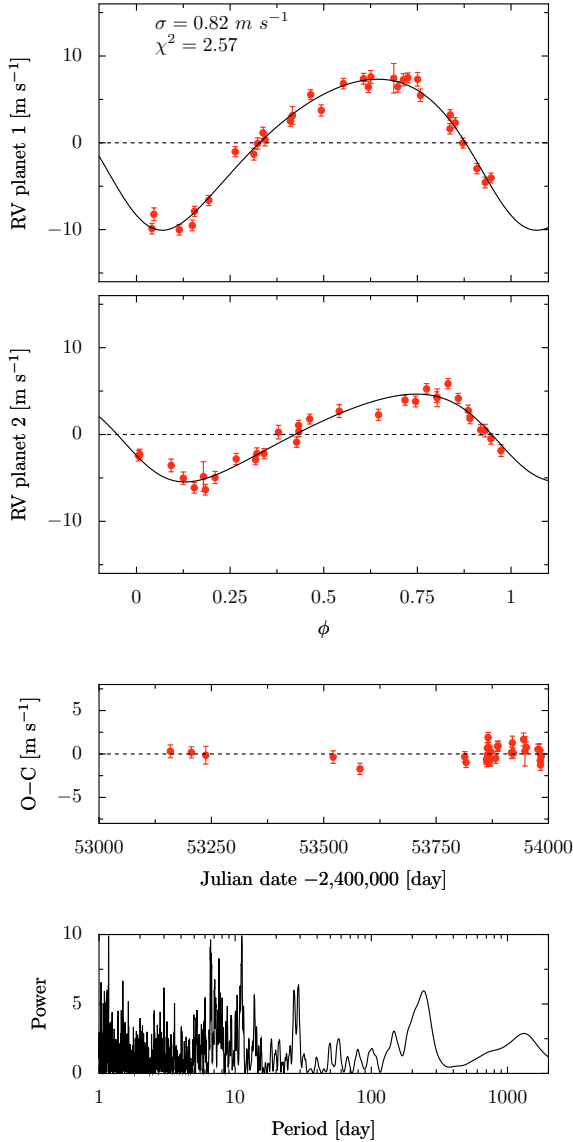
Fig. 4. *Top two panels*: radial velocity measurements phased to each of the two periods, after subtraction of the other component of our best 2-planet Keplerian model. *Third panel*: residuals of the best 2-planet fit as a function of time (O−C, Observed minus Computed). *Bottom panel*: lomb-Scargle periodogram of these residuals.

of the second signal a priori uncertain, and the very small rotation velocity removes much of the power of the usual bisector test (Appendix A). We therefore investigated its magnetic activity through photometric observations (Sect. 5.1) and detailed examination of the chromospheric features in the clean HARPS spectra (Sect. 5.2).

5.1. Photometric variability

We obtained photometric measurements with the CCD camera of the Euler Telescope (La Silla) during 21 nights between September 2 and October 19, 2006. GJ 674 was observed through a *VG* filter that, among those available, optimizes the flux ratio between GJ 674 and its two brightest reference stars. This relatively blue filters also happens to have good sensitivity to spots on cool stars such as GJ 674. To minimize atmospheric scintillation noise, we took advantage of the low stellar density to defocus the images to *FWHM* ∼ 11″, so that
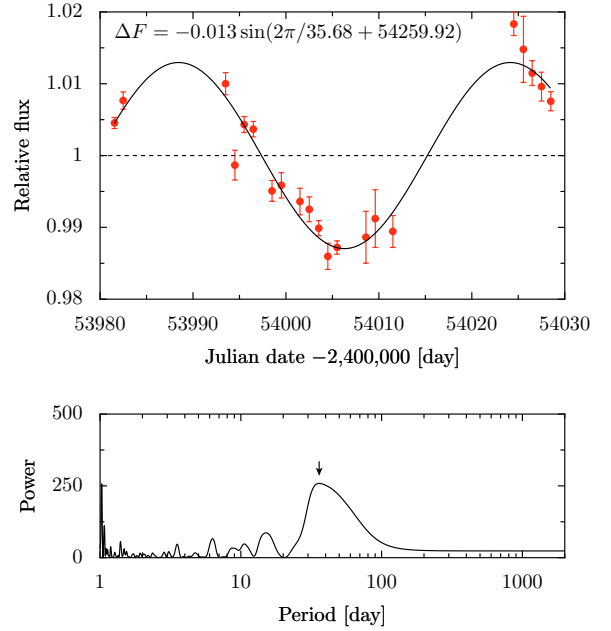

Fig. 5. *Upper panel*: differential photometry of GJ 674 as a function of time. The star clearly varies with a 1.3% amplitude. *Bottom panel*: the periodogram of the GJ 674 photometry exhibits significant power excess peaking at 35 days (small black arrow).

we could use longer exposure times. The increased read-out and sky-background noises from the larger synthetic aperture, which we then had to use, remain negligible compared to both stellar photon noise and scintillation.

We gathered 14 to 75 images per night with a median exposure time of 20 s. We used the Sept. 24th data, which have the longest nightly time base, to tune the parameters of the IRAF DAOPHOT package and optimise the set of reference stars (HD 157931, CD 4611534, and 7 anonymous fainter stars) to minimise the dispersion in the GJ 674 photometry for that night. These parameters were then fixed for analysis of the full data set. The nightly light curves for GJ 674 were normalized by that of the sum of the references, clipped at 3-σ to remove a small number of outliers, and then averaged to one measurement per night to examine the long-term photometric variability of GJ 674. GJ 674 clearly varies with a ∼1.3% amplitude and a (quasi-)period close to 35 days (Fig. 5). To verify that this variability does not actually originate in one of the reference stars, we repeated the analysis alternately using HD 157931 alone as the reference star and the average of the 8 other references. Both light curves are very similar to Fig. 5.

The photometric observations are consistent with the signal of a single spot, within the limitations of their incomplete phase coverage: the variations are approximately sinusoidal, and their ∼0.2–0.3 radian phase shift from the corresponding radial velocity signal closely matches the difference expected for a spot. The spot would cover 2.6% of the stellar surface if completely dark, corresponding to a ∼0.16 $R_\star$ radius for a circular spot.

5.2. Variability of the spectroscopic indices

The emission reversal in the core of the Ca II H&K resonant lines results from non-radiative heating of the chromosphere, which is closely coupled to spots and plages through magnetic connections between the photosphere and chromosphere. The Hα line is similarly sensitive to chromospheric activity. We
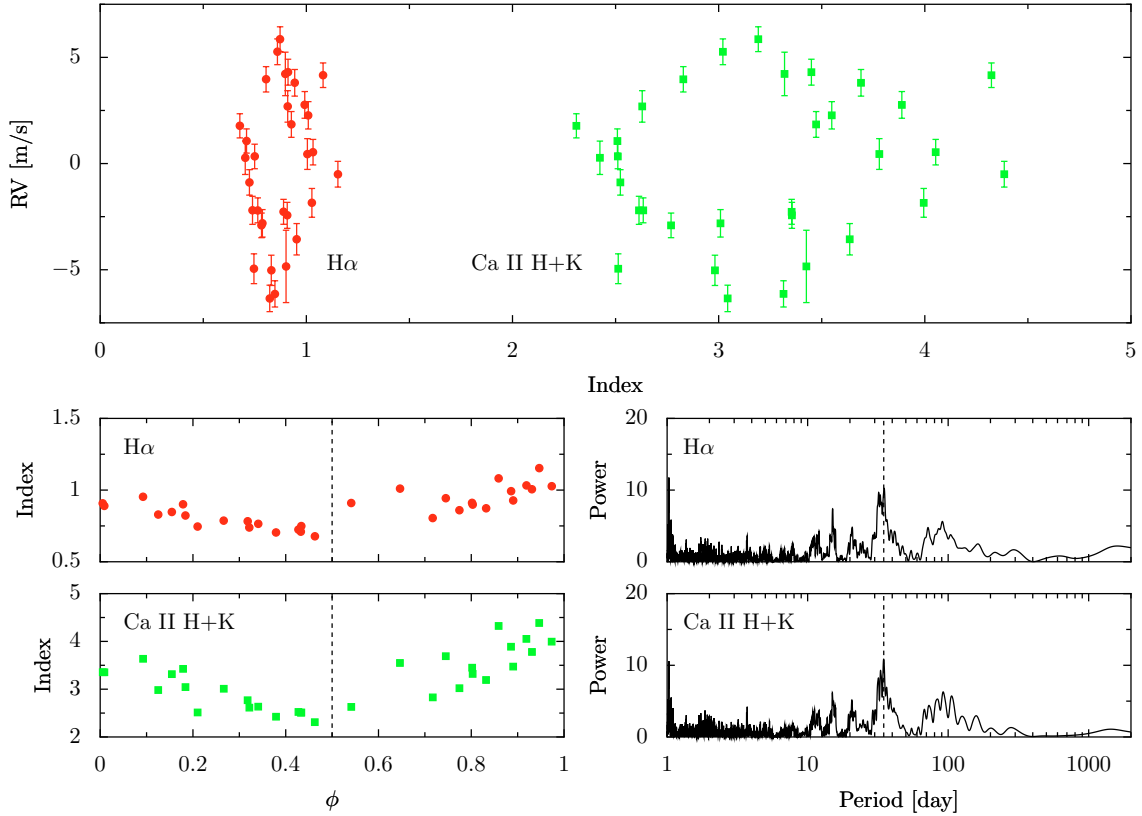
Fig. 6. *Upper panel*: differential radial velocity of GJ 674, corrected for the signature of the 4.69 days planet in our 2-planet Keplerian fit, as a function of the Hα (red filled circles) and Ca II H&K (green filled squares) spectral indices defined in the text. *Bottom right panels*: the Ca II H+K and Hα indexes phased to the longer period of the 2-planet keplerian model. *Bottom left panels:* Power density spectra of the spectroscopic indexes. A clear power excess peaks at 34.8 days (vertical dashed lines).

measured these chromospheric spectral-feature results in the clean HARPS spectra, used to measure the radial velocities, and examined their variability.

Like the well-known Mt. Wilson S index (Baliunas et al. 1995), our Ca II H+K index is defined as

$$\text{Index} = \frac{H + K}{B + V}, \tag{1}$$

with H and K sampling the two lines of the Ca II doublet, and B and V the continuum on both sides of the doublet. Our H and K intervals are 31 km s^{-1} wide and centered on 3933.664 and 3968.47 Å, while B and V are respectively integrated over [3952.6, 3956 Å] and [3974.8, 3976 Å].

This H+K index varies with a clear period of ~34.8 days (Fig. 6). Within the combined errors, this is consistent with both the photometric period and the longer radial-velocity period. The phasing of the chromospheric index and the photometry is such that lower photometric flux matches higher Ca II emission, as expected if active chromospheric regions hover over photospheric spots.

The imprint of a spot is also seen when the radial-velocity is plotted as a function of the spectral index value. During a star's rotation, the spot crosses the sub-observer meridian two times, once on the hemisphere facing the observer (with a maximal projected area) and once on the opposite hemisphere (with a minimal projected area, and possibly unseen because of its latitude and/or the stellar inclination). Since the rotational velocity cancels on the sub-observer meridian, the phases with index extrema correspond to radial-velocity minima. At intermediate phases, the spot induces positive or negative radial-velocity

shifts depending if the masked area is on a rotationally blue- or red-shifted part of the star. At the end of the day, the spectral index traces a closed loop as a function of radial velocity.

Chromospheric filling-in of the photospheric Hα absorption has similarly been found to be a powerful activity diagnostic for M dwarfs. Kürster et al. (2003) find that in Barnard's star it correlates linearly with the radial-velocity variations and interpret that finding as evidence that active plage regions inhibit the convective velocity field. The variation pattern in GJ 674 definitely differs from a linear correlation between Hα and the radial-velocity residuals, so it needs a different explanation.

Similar to Kürster et al. (2003), we define our Hα index as

$$\text{Index} = \frac{F_{\text{H}\alpha}}{F_1 + F_2}, \tag{2}$$

with $F_{\text{H}\alpha}$ sampling the Hα line, and F_1 and F_2 the continuum on both sides of the line. Our $F_{\text{H}\alpha}$ interval is 31 km s^{-1} wide and centered on 6562.808 Å, while F_1 and F_2 are integrated respectively over [6545.495, 6556.245 Å] and [6575.934, 6584.684 Å]. The Hα index behaves in a similar way to the Ca II H+K index.

The chromospheric indices vary by factors of ~2 and ~1.3 (for our specific choices of continuum windows) and are thus much more contrasted than the photometry. They do not, however, vary as smoothly with phase as the photometry, perhaps due to (micro-)flares, somewhat reducing their value as diagnostics of spot-induced radial velocity variations. These measurements on the other hand require no new observation, and they undoubtly reinforce the spot interpretation.

5.3. Planets vs. activity

In Sect. 4 we have shown that our 32 radial-velocity measurements of GJ 674 are described well by two Keplerian signals, as illustrated by the low reduced chi-square of that model. The above analysis (Sect. 5) however demonstrates that the rotation period of GJ 674 coincides with the longer of the two Keplerian periods. Both the stellar flux and the Ca II H+K emission vary with that period, implying that the surface of GJ 674 has a magnetic spot. This spot must induce radial-velocity changes, with the observed phase relative to the photometric signal. As a consequence, some, and probably all, of the 35-day radial-velocity signal must originate in the spot. Planet-induced activity through magnetic coupling (e.g. Shkolnik et al. 2005) should be an alternative explanation of the correlation, but here it is not a very attractive one: the inner planet is at least as massive as the hypothetical 35-day planet and would, at least naively, be expected to have stronger interactions with the magnetosphere of GJ 674. The 4.69-day period, however, is only seen in the radial velocity signal, and it has no photometric or chromospheric counterpart.

6. Discussion

6.1. Characteristics of GJ 674b

Perhaps the most important result of the above analysis is that the ~4.69-day planet of GJ 674 is robust: variability identifies the stellar rotation period as ~35 days, and the 4.69-day period therefore cannot reflect rotation modulation. In spite of its larger amplitude, the short period signal also has no counterpart in either photometry or chromospheric emission, further excluding a signal caused by magnetic activity.

The 1-planet fit, which effectively treats the activity signal as white noise, results in a minimum mass of $m_2 \sin i = 12.7\ M_\oplus$ for GJ 674b. The 2-planet fit by contrast filters out this signal. That filtering obviously uses a physical model that is not completely appropriate, but that remains preferable to handling a (partly) coherent signal as white noise. We therefore adopt the corresponding estimate of the minimum mass, $m_2 \sin i = 11.09\ M_\oplus$.

At 0.039 AU from its parent star, the temperature of GJ 674 b is ~450 K. Planets above a few Earth masses planets can, but need not, accrete a large gas fraction, leaving its composition – whether mostly gaseous or mostly rocky – unclear. The orbital eccentricity might shed light on the structure of GJ 674b, if confirmed by additional measurements. Rocky and gaseous planets have rather different dissipation properties, and significant eccentricity at the short period of GJ 674 b needs a high Q factor, unless it is pumped by an additional planet at a longer period (e.g. Adams & Laughlin 2006). For now, the stellar activity leaves the statistical significance of the eccentricity slightly uncertain, so we prefer to stay clear of overinterpreting it.

6.2. Properties of M-dwarf planets

One important motivation in searching for planets around M dwarfs is to investigate whether the planet-metallicity correlation found for Jupiter-mass planets around solar-type stars extends to very low-mass stars. Our photometric calibration of M dwarf metallicity (Bonfils et al. 2005b) gives respective metallicities of [Fe/H] = −0.03, −0.25, +0.14, +0.03, and −0.28 for GJ 436, GJ 581, GJ 849, GJ 876, and GJ 674. M dwarfs with known planets, an average metallicity of −0.078 and a median of −0.03. By comparison, the 44 M dwarfs of the
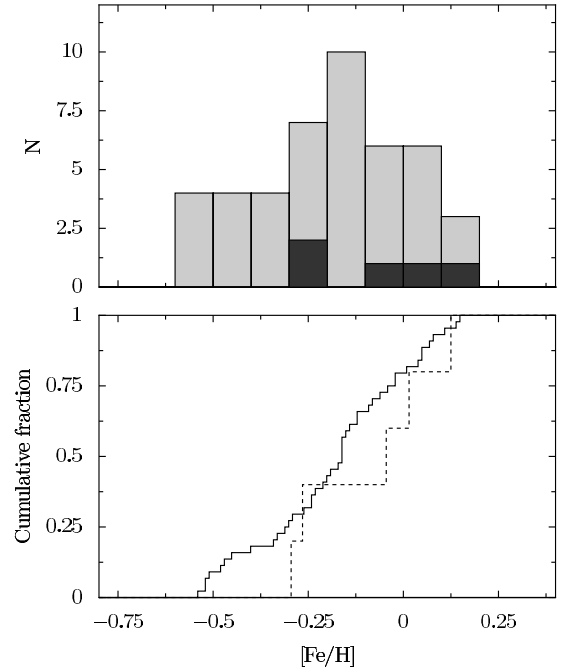

Fig. 7. *Upper panel*: metallicity distributions of 44 M dwarfs without known planets (gray shading) and of the 5 M dwarfs known to host planets (black shading). *Bottom panel*: corresponding cumulative distributions (solid and dashed lines, respectively).

Bonfils et al. (2005b) volume-limited sample, which are not currently known to host a planet, have average and median metallicities of −0.181 and −0.160. The M dwarfs with planets therefore appear slightly more metal-rich than M dwarfs without planets. A Kolmogorov-Smirnov test (Press et al. 1992) of the two samples gives an 11% probability that they are drawn from the same distribution. The significance of the discrepancy is therefore still modest, limited by small number statistics.

One can additionally note that the two stars that host giant planets, GJ 876 and GJ 849, occupy the metal-rich tail of the M dwarf metallicity distribution, with GJ 849 almost as metal-rich as the most metal-rich star of the comparison sample. The next most metal-rich of the M dwarfs with planets, GJ 436, has an additional long-period companion ($P > 6$ yr) that might well be a giant planet (Maness et al. 2006), which would then strengthen that trend. If confirmed by additional data, this would validate the theoretical predictions (Ida & Lin 2004; Benz et al. 2006) that only Jovian-mass planets are more likely to form around metal-rich stars. Current observations are consistent with this prediction, but not yet very conclusively so (Udry et al. 2006).

Much recent theoretical work has gone into examining how planet formation depends on stellar mass. Within the "core accretion" paradigm, Laughlin et al. (2004) and Ida & Lin (2005) predict that giant planet formation is inhibited around very low-mass stars, while Neptune-mass planets should inversely be common. Within the same paradigm, but assuming that M dwarfs have denser protoplanetary disks, Kornet et al. (2006) predict instead that Jupiter-mass planets become more frequent in inverse proportion to the stellar mass. Finally, Boss (2006) examines how planet formation depends on stellar mass for planets formed by disk instability, and concludes that the frequency of Jupiter-mass planets is independent of stellar mass, as long as disks are massive enough to become unstable.

Table 2. Keplerian parameterization for GJ 674b and GJ 674's spot.

Parameter		GJ 674b	Spot
P	[days]	4.6938 ± 0.007	34.8467 ± 0.0324
T	[JD]	$2\,453\,780.085 \pm 0.078$	$2\,453\,767.13 \pm 0.92$
e		0.20 ± 0.02	0.20 ± 0.05
ω	[deg]	143 ± 6	113 ± 9
K	[m s^{-1}]	8.70 ± 0.19	5.06 ± 0.19
$a_1 \sin i$	[AU]	$3.68\ 10^{-6}$	1.59×10^{-5}
$f(m)$	[$M_\odot$]	$3.0\ 10^{-13}$	4.4×10^{-13}
$m_2 \sin i$	[M_{Earth}]	11.09	12.58
a	[AU]	0.039	0.147

To date, none of the ~300 M dwarfs scrutinized for planets by the various radial-velocity searches (Bonfils et al. 2006; Endl et al. 2006; Butler et al. 2006) has been found to host a hot Jupiter. Conversely, GJ 674b is already the 4th hot Neptune. Although that cannot be established quantitatively yet, these surveys are likely to be almost complete for hot jupiters, which are easily detected. Hot-Neptune detection, on the other hand, is definitely very incomplete. Setting aside this incompleteness for now, simple binomial statistics show that the probability of finding none and 4 detections in 300 draws of the same function is only 3%. There is thus a 97% probability that hot Neptunes are more frequent than hot Jupiters around M dwarfs. Accounting for this detection bias in more realistic simulations (Bonfils et al. in prep.) obviously increases the significance of the difference. Planet statistics around M dwarfs therefore favor the theoretical models that, at short periods, predict more Neptune-mass planets than Jupiter-mass planets.
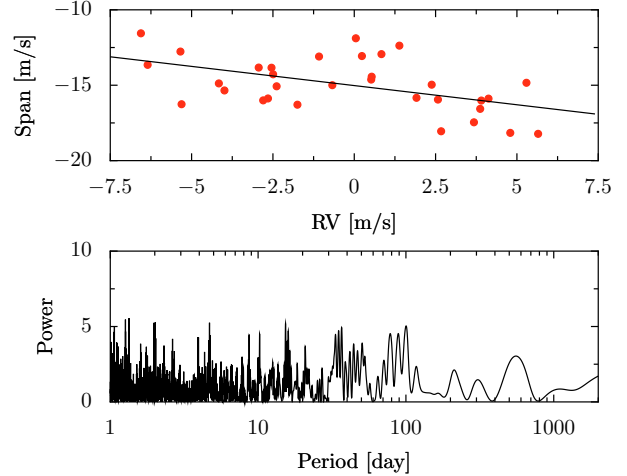
Appendix A: Bisector analysis

As demonstrated by Saar & Donahue (1997), the bisector analysis loses much of its diagnostic power when applied to slow rotators. In simulations of the impact of star spots on radial-velocity and bisector measurements, they found that, for a given spot configuration, the radial velocity varies linearly with $v \sin i$, while the bissector span varies as $(v \sin i)^{3.3}$. The bissector signal therefore decreases faster with decreasing rotational velocities than the radial-velocity signal, and disapears faster in measurement noise. For GJ 674 we measure a very low rotation velocity ($v \sin i < 1$ km s^{-1}). It is therefore not surprising that the correlation between the bissector span and radial velocity is weak (Fig. A.1) and not statistically significant.

Fig. A.1. Bisector analysis for GJ 674 measurements.

References

Adams, F. C., & Laughlin, G. 2006, ApJ, 649, 1004
Baliunas, S. L., Donahue, R. A., Soon, W. H., et al. 1995, ApJ, 438, 269
Beaulieu, J.-P., Bennett, D. P., Fouqué, P., et al. 2006, Nature, 439, 437
Bennett, D. P., Anderson, J., Bond, I. A., Udalski, A., & Gould, A. 2006, ApJ, 647, L171
Benz, W., Mordasini, C., Alibert, Y., & Naef, D. 2006, in Tenth Anniversary of 51 Peg-b: Status of and prospects for hot Jupiter studies, ed. L. Arnold, F. Bouchy, & C. Moutou, 24
Bond, I. A., Udalski, A., Jaroszyński, M., et al. 2004, ApJ, 606, L155
Bonfils, X., Delfosse, X., Udry, S., et al. 2005a, A&A, 442, 635
Bonfils, X., Forveille, T., Delfosse, X., et al. 2005b, A&A, 443, L15
Bonfils, X., Delfosse, X., Udry, S., Forveille, T., & Naef, D. 2006, in Tenth Anniversary of 51 Peg-b: Status of and prospects for hot Jupiter studies, ed. L. Arnold, F. Bouchy, & C. Moutou, 111
Boss, A. P. 2006, ApJ, 643, 501
Bouchy, F., Pepe, F., & Queloz, D. 2001, A&A, 374, 733
Butler, R. P., Vogt, S. S., Marcy, G. W., et al. 2004, ApJ, 617, 580
Butler, R. P., Johnson, J. A., Marcy, G. W., et al. 2006, ArXiv Astrophysics e-prints
Cutri, R. M., Skrutskie, M. F., van Dyk, S., et al. 2003, 2MASS All Sky Catalog of point sources, The IRSA 2MASS All-Sky Point Source Catalog, NASA/IPAC Infrared Science Archive, http://irsa.ipac.caltech.edu/applications/Gator/
Delfosse, X., Forveille, T., Mayor, M., et al. 1998, A&A, 338, L67
Delfosse, X., Forveille, T., Ségransan, D., et al. 2000, A&A, 364, 217
Endl, M., Cochran, W. D., Kürster, M., et al. 2006, ApJ, 649, 436
ESA. 1997, VizieR Online Data Catalog, 1239, 0
Gould, A., Udalski, A., An, D., et al. 2006, ApJ, 644, L37
Hawley, S. L., Gizis, J. E., & Reid, N. I. 1997, AJ, 113, 1458
Hünsch, M., Schmitt, J. H. M. M., Sterzik, M. F., & Voges, W. 1999, Late-type stars in the ROSAT all-sky survey, ed. B. Aschenbach, & M. J. Freyberg, 387
Ida, S., & Lin, D. N. C. 2004, ApJ, 604, 388
Ida, S., & Lin, D. N. C. 2005, ApJ, 626, 1045
Kornet, K., Wolf, S., & Różyczka, M. 2006, A&A, 458, 661
Kürster, M., Endl, M., Rouesnel, F., et al. 2003, A&A, 403, 1077
Laughlin, G., Bodenheimer, P., & Adams, F. C. 2004, ApJ, 612, L73
Leggett, S. K. 1992, ApJS, 82, 351
Leggett, S. K., Allard, F., Geballe, T. R., Hauschildt, P. H., & Schweitzer, A. 2001, ApJ, 548, 908
Lovis, C., & Pepe, F. 2007, ArXiv Astrophysics e-prints
Lovis, C., Mayor, M., Pepe, F., et al. 2006, Nature, 441, 305
Maness, H. L., Marcy, G. W., Ford, E. B., et al. 2006, ArXiv Astrophysics e-prints
Marcy, G. W., Butler, R. P., Vogt, S. S., Fischer, D., & Lissauer, J. J. 1998, ApJ, 505, L147
Marcy, G. W., Butler, R. P., Fischer, D., et al. 2001, ApJ, 556, 296
Mayor, M., Pepe, F., Queloz, D., et al. 2003, The Messenger, 114, 20
McArthur, B. E., Endl, M., Cochran, W. D., et al. 2004, ApJ, 614, L81
Pepe, F., Mayor, M., Queloz, D., et al. 2004, A&A, 423, 385
Press, W. H., Teukolsky, S. A., Vetterling, W. T., & Flannery, B. P. 1992, Numerical recipes in C. The art of scientific computing, 2nd (Cambridge: University Press)
Queloz, D., Henry, G. W., Sivan, J. P., et al. 2001, A&A, 379, 279
Rivera, E. J., Lissauer, J. J., Butler, R. P., et al. 2005, ApJ, 634, 625
Saar, S. H., & Donahue, R. A. 1997, ApJ, 485, 319
Santos, N. C., Bouchy, F., Mayor, M., et al. 2004, A&A, 426, L19
Shkolnik, E., Walker, G. A. H., Bohlender, D. A., Gu, P.-G., & Kürster, M. 2005, ApJ, 622, 1075
Turon, C., Creze, M., Egret, D., et al. 1993, Bulletin d'Information du Centre de Donnees Stellaires, 43, 5
Udalski, A., Jaroszyński, M., Paczyński, B., et al. 2005, ApJ, 628, L109
Udry, S., Mayor, M., Benz, W., et al. 2006, A&A, 447, 361